Medjunarodni naučno-stručni skup sa izložbom
XXI NAUKA I MOTORNA VOZILA SCIENCE AND MOTOR VEHICLES 2007
JUMV International Automotive Conference with Exhibition
23 - 25 April, Beograd, Serbia

Aerodynamic optimization of vehicles using computational fluid dynamics and response surface methodology

Siniša Krajnović
Department of Applied Mechanics, Chalmers University of Technology, Gothenburg, Sweden

Abstract:
The present paper investigates use of the surrogate models for the multi-objective shape optimization of vehicles. The objectives of interest are related to the aerodynamic performance of vehicles such as air resistance (drag), lift force, moments, aeroacoustic properties or soiling and accumulation of water. The suggested technique is tested here on a two-dimensional vehicle geometry with four design variables and two objective functions. Faced centered composite design is used to define the data points in the design space that will be used for the computer experiments (CFD) with a steady solver and standard k – ε turbulence model. The second order polynomial response surface model is then constructed from the computer calculated responses from CFD. Search for the optimal design is done using the ε-constraint method. In order to investigate the correlation between the two objectives (the drag and the lift) the Pareto-optimal solutions were computed. Hierarchical cluster algorithm is finally used to analyze the Pareto optimal solutions and to draw conclusions about the design. Finally some improvements of the technique that are required in order to make the suggested technique to become an engineering tool are discussed.

Keywords: Surrogate model, response surface, optimization, Pareto-optimal solution

INTRODUCTION

The optimization of the aerodynamics of road and rail vehicles has traditionally been handled through trial-and-error design procedures, which count on the skills and experience of the designer to suggest changes in the design that are likely to yield improvements. Although such a procedure usually yield an acceptable design and use of more rigorous optimization methodology would allow the best design to be identified. The majority of numerical design optimization in fluid machinery uses gradient-based search algorithms. These methods work iteratively through the design space until the optimal design is reached. Such an approach is impractical in optimization of vehicle aerodynamics due to computational effort required for such a large number of CFD simulations.

One way of making the shape optimization of the vehicle feasible is to use the surrogate model based optimization to estimate the response of CFD simulation. These models have been used successfully in various fields such as design of airfoils, propulsion and turbo machinery. The surrogate models give a global approximation of the response and therefore can be used in providing better understanding of the relationship between the design variables and the response. There are several different surrogate models such as response surfaces (polynomial regressions), neural network, Kriging and Radial Basis Functions. Here we shall only discuss the response surface model that was used in the present study. The design problem of vehicle aerodynamics has multiple objectives, i.e. drag, lift force, cross-wind stability, aeroacoustics etc. Such a multi-objective optimization problem has several optimal solutions called the Pareto optimal front which can help the designers to visualize the trade-offs between different objectives and select an compromise design.

The present work presents the use of response surface approximation (RSA) for multi-objective optimization of vehicle aerodynamics. We use an example of optimization of aerodynamic properties of a two-dimensional vehicle to demonstrate an efficient multi-objective optimization procedure. The chosen object functions are drag and lift and the response surfaces are produced as a result of Reynolds-Averaged Navier-Stokes simulations (RANS) using simple two equation turbulence model.

Surrogate modeling

The surrogate modeling aims to determine a continuous function $f(\boldsymbol{x})$ of a set of design variables $\boldsymbol{x} = (x_1, x_2, ..., x_N)$ from relatively small amount of available data $g(\boldsymbol{x})$ in form of computer calculated response.
Having a true response given as:

$$y = f(\boldsymbol{x}) \tag{1}$$

a surrogate model of the true response is given by:

$$\hat{y} = g(\boldsymbol{x}) \tag{2}$$

with $y = \hat{y} + \varepsilon$. The error ε consist of the modeling error and the measurement error which is random. In the numerical experiments (simulations) the modeling error is a result of the choice of the lack of surrogate model approximation while the measurement error is the numerical error.

The optimization process using surrogate models

There are five steps in optimization using surrogate models:
1. *Geometric parameterization.* First step of every shape design process is to choose design variables. Keeping the number of design variables as low as possible is important for the computational cost of the design procedure. Vehicle shapes are today quantified using modern computer aided design (CAD) models and their description can be presented using complex mathematical description (using B-splines). It is better for an optimization purpose if the shape can be described with traditional design variables such as height, length, radius etc., which can then be translated by the computer into a CAD model. However there is today no optimal way to quantify shapes of ground vehicles today and different choices of design variables have to be compared against each other in order to find the best parameterization.
2. *Design of experiments (DOE).* A design of experiment is a sequence of experiments (numerical experiments in our case) that will be performed. This is a critical step as the quality of the response surface approximation is dependent on the choice of the points in the design variable space from which the model will be constructed. There are several different design strategies (for the review see e.g.[1] and here the Faced Centered Composite Design (FCCD) is chosen to pick the design data points.
3. *Numerical simulation at design points.* Here the CFD simulations of the designs chosen in DOE are performed. This is the most costly step (in terms of both computational resources and the men power) in the optimization process and consist of preprocessing (making computational meshes), numerical calculations and post-processing (analysis of the results). The choice of the numerical method (numerical scheme, turbulence model, steady or unsteady solver) is essential for the success of the optimization process as the computer calculated response is used for the construction of the surrogate model.
4. *Construction of the surrogate model.* In this step a surrogate model is constructed from the relationship between the design variables and the computer calculated response. There are several different surrogate models and here we shall only discuss the polynomial response surfaces.
5.*Search for the optimal design.* When the surrogate model is constructed a search for the optimal design can be initiated. In the case of only one objective the optimization process is a simple minimization problem. This can also be done in a case of multi-objective optimization where one minimizes one objective and uses other objectives as a inequality constrains. However more convenient in the case of multi-objective optimization is to determine so called Pareto-optimal solutions. In the present work we shall do both.

1. Geometric parameterization of the train

In the present paper we chose to describe the shape of the front of the train using four length variables. This is by no means the optimal description but is sufficient for the purpose of our investigation of surrogate models in optimization process.

The geometry of the train is presented in Fig. 1. The length and the height of the car are chosen as $B = 20$m and $H = 3$m, respectively. The ground clearance is $c = 0.4$m. The objective of the present work is the aerodynamic optimization of the nose of the train shown in Fig. 2.

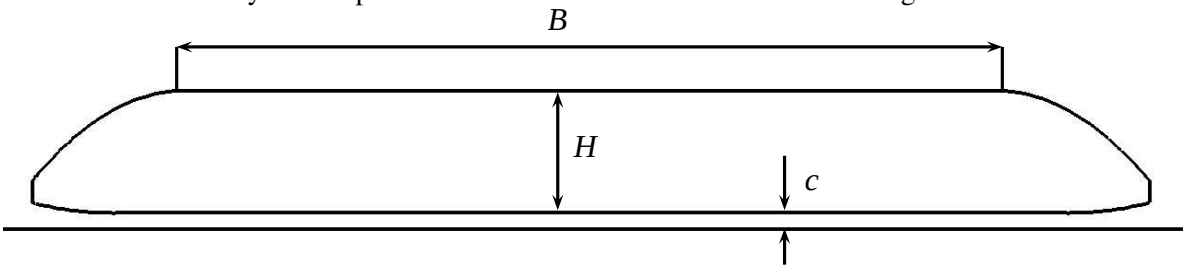

Figure 1: Geometry of the train

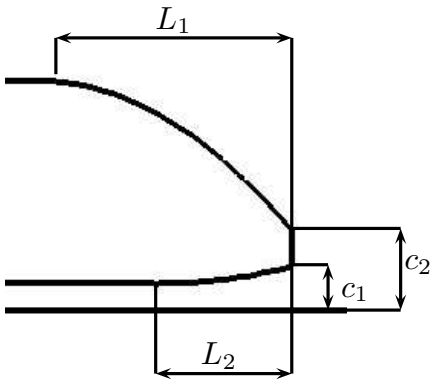

Figure 2: Geometry of the nose of the train.

There are four design variables for the nose of the train shown in this figure, L_1, L_2, c_1 and c_2. These are chosen to vary between $2.5m \leq L_1 \leq 5m$, $0.5m \leq L_2 \leq 2m$, $0.5m \leq c_1 \leq 0.8m$ and $0.9m \leq c_2 \leq 1.5m$. These four design parameters are used for the description of the front of the train defined with two parabolic curves:

$$\begin{aligned} y &= (c_2 - 3.4)/L_1^2 x^2 + 20(3.4 - c_2)L_1^2 x + 3.4 - (340 - 100c_2)/L_1^2 \\ y &= (0.4 - c_1)/L_2^2[x^2 - 2(10 + L_1 - L_2)x + L_2^2/(0.4 - c_1)c_1 - (100 + 20L_1 + L_1^1) \\ &+ 2(10 + L_1)(10 + L_1 - L_2)] \end{aligned} \tag{3}$$

2. Design of experiments

In the present study we are using center composite design (CCD). This DOE was originally constructed for physical experiments but is often used for the design of computer experiments. CCD is a two level factorial design containing two 'star' points at $\pm\alpha$ for each factor and n center points. In the case of three design variables we have that the 'star' points are located in the center of the faces of the cube resulting in a so called Faced Centered Composite Design (FCCD). This technique generates $2^N + 2N + 1$ design points, where N is the number of design variables. This is the main drawback of this DOE as the number of design points increases fast with the number of the design variables. In our case of four design variables a total of 25 design points were obtained which is a manageable number of designs. These designs are presented in Table 1 using both the natural and the coded variables.

Case	L_1	L_2	c_1	c_2	x_1	x_2	x_3	x_4	y_d	y_l
1	2.5	0.5	0.5	0.9	-1	-1	-1	-1	0.2987	0.1894
2	2.5	0.5	0.5	1.5	-1	-1	-1	1	0.2673	0.2588
3	2.5	0.5	0.8	0.9	-1	-1	1	-1	0.3051	0.2602
4	2.5	0.5	0.8	1.5	-1	-1	1	1	0.2674	0.3690
5	2.5	2.0	0.5	0.9	-1	1	-1	-1	0.3105	0.2217
6	2.5	2.0	0.5	1.5	-1	1	-1	1	0.2766	0.2872
7	2.5	2.0	0.8	0.9	-1	1	1	-1	0.3527	0.0088
8	2.5	2.0	0.8	1.5	-1	1	1	1	0.3175	0.0847
9	5.0	0.5	0.5	0.9	1	-1	-1	-1	0.1455	0.4234
10	5.0	0.5	0.5	1.5	1	-1	-1	1	0.1693	0.4531
11	5.0	0.5	0.8	0.9	1	-1	1	-1	0.1488	0.5103
12	5.0	0.5	0.8	1.5	1	-1	1	1	0.1746	0.5564
13	5.0	2.0	0.5	0.9	1	1	-1	-1	0.1477	0.4483
14	5.0	2.0	0.5	1.5	1	1	-1	1	0.1724	0.4752
15	5.0	2.0	0.8	0.9	1	1	1	-1	0.1723	0.2836
16	5.0	2.0	0.8	1.5	1	1	1	1	0.1973	0.3131
17	2.5	1.25	0.65	1.2	-1	0	0	0	0.3028	0.0971
18	5.0	1.25	0.65	1.2	1	0	0	0	0.1622	0.3407
19	3.75	0.5	0.65	1.2	0	-1	0	0	0.1866	0.4220
20	3.75	2.0	0.65	1.2	0	1	0	0	0.2091	0.2316
21	3.75	1.25	0.5	1.2	0	0	-1	0	0.1878	0.3844
22	3.75	1.25	0.8	1.2	0	0	1	0	0.2042	0.2998
23	3.75	1.25	0.65	0.9	0	0	0	-1	0.2052	0.2264
24	3.75	1.25	0.65	1.5	0	0	0	1	0.2026	0.2999
25	3.75	1.25	0.65	1.2	0	0	0	0	0.2024	0.2593

Table 1: Faced Central Composite Design for design of the nose of the train.

3. Numerical computations at the design points

Prediction of the drag and lift coefficients is very much dependent on the numerical method used for the simulation. These two aerodynamic forces for road and the rail vehicles are mainly the result of the wake flow behind vehicles. However the wake flow being unsteady and containing wide spectrum of turbulent scales is difficult to predict with steady numerical methods such as RANS. Unsteady numerical methods such as large eddy simulations (LES) [2, 3, 4, 5, 6, 7], detached eddy simulations (DES) or hybrid LES-RANS techniques are better equipped to predict this complex flow. Unfortunately these time-dependent techniques are computationally intensive and are still at the testing stage in industry. As the RANS methods are widely used in industry we shall adapt this approach here keeping in mind that the prediction of aerodynamic forces is only qualitative. Although the RANS technique can use large number of turbulent models developed during last four decades which often produce large differences in the quality of predictions, we shall here use simple $k-\varepsilon$ model with wall functions. It is possible that use of some other turbulence model would result in different optimal solution but the topic of the present work is the optimization using surrogate models and we leave the choice of the appropriate turbulence model or even the simulation approach (steady or unsteady) for a future investigation.

All the CFD simulations in the present work are performed using commercial software FLUENT. The convective fluxes are discretized using second order upwind scheme and the simulations were stopped first when all the residuals have settled down below approximately 10^{-6}. At the inlet and on the ground a velocity equal to 200 km/h was used as a boundary condition. The roof of the computational domain was treated as a symmetry boundary condition while the homogeneous Neumann boundary condition was used at the outlet. The first node from the surface of the train was located between $50 \leq y^+ \leq 100$ (i.e. in the logarithmic law region) in all computational grids. y^+ is here the wall-normal distance expressed in wall units, i.e. $y^+ = u_* y/\nu$ with u_* being the friction velocity.

4. Response surface surrogate models

A second-order polynomial model of the response surface is used as a surrogate model for both objective functions, the lift and the drag. This model has the following form:

$$\hat{y} = \beta_0 + \sum_{i=1}^{n} \beta_i x_i + \sum_{i=1}^{n} \sum_{j<i}^{n} \beta_{ij} x_i x_j + \sum_{i=1}^{n} \beta_{ii} {x_i}^2 \tag{4}$$

where n is the number of design variables.

In our case of four design variables the model has the form:

$$\begin{aligned} \hat{y} &= \beta_0 + \beta_1 x_1 + \beta_2 x_2 + \beta_3 x_3 + \beta_4 x_4 + \beta_{12} x_1 x_2 + \beta_{13} x_1 x_3 + \beta_{14} x_1 x_4 \\ &+ \beta_{23} x_2 x_3 + \beta_{24} x_2 x_4 + \beta_{34} x_3 x_4 + \beta_{11} x_1^2 + \beta_{22} x_2^2 + \beta_{33} x_3^2 + \beta_{44} x_4^2 \end{aligned} \tag{5}$$

5. Variable selection

The response surface $\hat{y}$ is fit to the data y_l and y_d in Table 1 using the least square fit. In order to measure the goodness of the fit we use both the coefficient of multiple determination R^2 and R-square adjusted (R_a^2).

The coefficient of multiple determination R^2 measures the fraction of variation in data captured by response surface.

$$R^2 = SS_R/SS_T = 1 - SS_E/SS_T \tag{6}$$

where SS_E is the sum of squared approximation errors at the n_p sampling points, SS_T is the true response's sum of squared variations from the mean $\bar{y}$, and SS_R is the approximation's sum of squared variations from the mean, i.e.

$$SS_E = \sum_{i=1}^{n_p} (y_i - \hat{y}_i)^2, \quad SS_T = \sum_{i=1}^{n_p} (y_i - \bar{y}_i)^2, \quad SS_R = SS_T - SS_E = \sum_{i=1}^{n_p} (\hat{y}_i - \bar{y}_i)^2 \tag{7}$$

Coefficient	t (full)	$t\ (-b_{24})$	$t\ (-b_{34})$	$t\ (-b_{22})$	$t\ (-b_{33})$
b_0	130.8399	137.2257	142.3318	147.4471	138.7281
b_1	-80.5528	-84.4843	-87.6279	-89.2458	-81.5026
b_2	12.8511	13.4783	13.9799	14.2380	13.0026
b_3	10.9381	11.4720	11.8988	12.1185	11.0671
b_4	-2.7662	-2.9012	-3.0092	-3.0647	-2.7988
b_{12}	-4.7580	-4.9902	-5.1759	-5.2715	-4.8141
b_{13}	-2.2270	-2.3357	-2.4226	-2.4673	-2.2533
b_{14}	16.7909	17.6104	18.2657	18.6029	16.9889
b_{23}	8.3071	8.7125	9.0367	9.2035	8.4050
b_{24}	0.0071	——	——	——-	——
b_{34}	-0.3747	-0.3930	——	——-	——
b_{11}	14.9664	15.6969	16.2810	17.0269	16.0611
b_{22}	-0.6711	-0.7038	-0.7300	———	——-
b_{33}	-1.5060	-1.5795	-1.6383	-1.9459	——
b_{44}	2.0593	2.1598	2.2401	2.1605	1.4079

Table 2: t statistics from linear regression analysis for the response surface approximation of the drag function.

A better suited measure for assessing predictive accuracy is the R-square adjusted (R_a^2) defined as

$$R_a^2 = 1 - \frac{SS_E/(n_p - n_\beta)}{SS_T/(n_p - 1)} \tag{8}$$

where n_β is the number of regression coefficients. Both R^2 and R_a^2 range between zero and one, and the higher value indicate better predicting accuracy of the response surface.
Although we first fit the full quadratic model, it is possible that this is not an appropriate model, i.e. it is possible that a model based on a subset of the regressors in the full model may be superior. In the present work, a backward elimination procedure based on the t statistic is used to discard terms and improve the prediction accuracy. The t statistics of the fitting coefficient is defined as its value divided by an estimate of the standard error of the coefficient.
In the backward elimination we begin with a model that includes all candidate regressors (i.e. full quadratic model in our case) and than the partial t statistic is computed for each regressors as if it were last variables to enter the model. The smallest of these partial t-statistics is compared with preselected value, t_{out} and if it is less than t_{out}, that regressor is removed from the model. Here, we chose $t_{out} = 2$ which is a common value for t_{out}. Tables 2 and 4 list t statistics of the regression coefficients b_i for the drag and the lift response surfaces, respectively.
The full quadratic response surface model $\hat{y}_d$ for the drag coefficient, has a R_a^2 of 0.9968. The t statistics presented in Table 2 suggests that the determination of the quadratic-term regressor b_{24} involves a large standard error. Discarding this term, the new regression analysis with a model of fourteen terms increased R_a^2 to 0.9971. In the same time, the R^2 value was unchanged between the full and the reduced model and was 0.9987. The backward elimination procedure for response surface approximation (RSA) was continued by removing of regressors b_{34}, b_{22} and b_{33}. Data on the elimination is presented in Table 2.
According to Table 2, removal of quadratic regressor b_{22} and mixed regressor b_{34} improved the standard errors of the remaining terms. Although the t statistics of the regressor b_{33} is less than 2, removal of this term decreased R_a^2 in Table 3. Thus further elimination of terms does not improve the fit and the best quadratic RSA of the drag is:

Removed regressors	R^2	R_a^2
—-	0.9987	0.9968
b_{24}	0.9987	0.9971
b_{34}	0.9987	0.9973
b_{22}	0.9986	0.9974
b_{33}	0.9982	0.9969

Table 3: Backward elimination procedure for response surface approximation of the drag function.

Coefficient	t (full)	$t\ (-b_{12})$	$t\ (-b_{24})$	$t\ (-b_{34})$	$t\ (-b_{44})$	$t\ (-b_{13})$
b_0	29.7575	30.6429	31.3528	31.6886	32.0802	31.5594
b_1	22.4646	23.1330	23.6689	23.9224	23.9280	23.5395
b_2	-12.0612	-12.4200	-12.7078	-12.8439	-12.8469	-12.6383
b_3	-5.0488	-5.1990	-5.3194	-5.3764	-5.3777	-5.2903
b_4	5.8212	5.9944	6.1332	6.1989	6.2004	6.0997
b_{12}	0.6112	——	——	——	——-	——-
b_{13}	1.1495	1.1837	1.2111	1.2241	1.2244	——
b_{14}	-2.2027	-2.2682	-2.3207	-2.3456	-2.3461	-2.3081
b_{23}	-13.0867	-13.4760	-13.7883	-13.9359	-13.9392	-13.7129
b_{24}	-0.6606	-0.6802	——	——-	——	——
b_{34}	0.8087	0.8327	0.8520	——-	——	——
b_{11}	-4.2561	-4.3827	-4.4843	-4.5323	-4.9962	-4.9151
b_{22}	3.8396	3.9538	4.0454	4.0888	3.9683	3.9039
b_{33}	4.9876	5.1359	5.2549	5.3112	5.2395	5.1544
b_{44}	-0.9360	-0.9639	-0.9862	-0.9968	——	——

Table 4: t statistics from linear regression analysis for the response surface approximation of the lift function.

$$\begin{aligned}\hat{y}_d &= 0.1996 - 0.0671x_1 + 0.0107x_2 + 0.0091x_3 - 0.0023x_4 - 0.0042x_1x_2 \\ &- 0.002x_1x_3 + 0.0148x_1x_4 + 0.0073x_2x_3 + 0.0328x_1^2 - 0.0037x_3^2 + 0.0042x_4^2\end{aligned} \tag{9}$$

Similar procedure of backward elimination is made for the response surface of lift. The t statistics and the results of the backward elimination are presented in Tables 4 and 5.
The RSA of the lift force coefficient has the following form

$$\begin{aligned}\hat{y}_l &= 0.2717 + 0.1126x_1 - 0.0605x_2 - 0.0253x_3 + 0.0292x_4 + 0.0061x_1x_3 \\ &- 0.0117x_1x_4 - 0.0696x_2x_3 - 0.0601x_1^2 + 0.0478x_2^2 + 0.0631x_3^2\end{aligned} \tag{10}$$

Multiple response optimization

In the present work, there are two responses, the lift and the drag, that we want to optimize. Here the ε-constraint method is used to solve the optimization problem as a constrained optimization problem. The C_D coefficient is chosen to be a primary response to be optimized and the lift coefficient response is expressed in the form of an inequality constraint

Removed regressors	R^2	R_a^2
—-	0.9896	0.9750
b_{12}	0.9892	0.9764
b_{24}	0.9887	0.9775
b_{34}	0.9881	0.9780
b_{44}	0.9871	0.9780
b_{13}	0.9858	0.9772

Table 5: Backward elimination procedure for response surface approximation of the lift function.

Population size	200
Generations	1000
Crossover probability	0.9
Distribution parameter (for crossover)	20
Mutation probability	0.25
Distribution parameter (for mutation)	20

Table 6: Parameters used for the NSGA−II simulation.

$$\begin{aligned} minimize \quad & C_D \\ subject \ \ to & \\ & C_L \leq \varepsilon \end{aligned} \tag{11}$$

There are several different numerical techniques that can be used to solve this problem and here the sequential quadratic programming in MATLAB is used to solve the optimization problem. For the purpose of validation of the optimization technique we have chosen the $\varepsilon = 0.3$. The minimization of C_D subject to $C_L \leq 0.3$ resulted in $C_{D_{min}} = 0.1575$ and $C_L = 0.3$ for the train with the coded variables $x_1 = 1.0$, $x_2 = 0.2398$, $x_3 = -0.1169$ and $x_1 = -1.0$ or expressed in natural variables $L_1 = 5.0$, $L_2 = 1.4299$, $c_1 = 0.6325$ and $c_2 = 0.9$.
Next step in validation of the suggested optimization procedure is to construct a new design described with these variables and perform a CFD simulation to evaluated the C_D and C_L values. The resulting values from the CFD simulation for the resulting design were $C_D = 0.1571$ and $C_L = 0.3041$. which are only 0.25% and 1.35% lower and higher, respectively, from the values found using response surface approximations.

Pareto optimal solutions

As a second step Pareto-optimal solutions were computed. A solution is called Pareto-optimal solution, if there is no other simulation for which at least one objective has better value while values of the remaining objectives are the same or better.

Multi-objective evolutionary algorithm

The two objective optimization problem was solved using a multi-objective evolutionary algorithm (MOEA) to find the Pareto optimal solution. The MOEA used here is so called real-coded NSGA−II algorithm by Deb *et al.* [8]. The parameters chosen for the NSGA −II simulation are presented in Table 6.
Further details on the NSGA−II algorithm can be found in [8]. The MOEA resulted in a Pareto optimal solutions shown in Fig. 3.

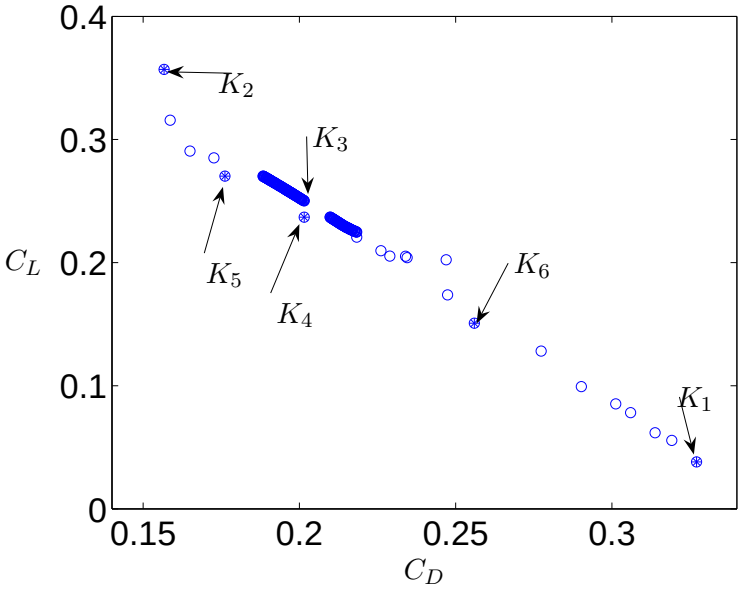

Figure 3: Pareto optimal solution front and six representative solutions from the same set. The * are the representatives of cluster K_i, $i = 1, 2, ..., 6$.

Case	L_1	L_2	c_1	c_2	x_1	x_2	x_3	x_4	$\hat{y}_d$	$\hat{y}_l$
K_1	2.5323	1.8338	0.7598	1.0525	-0.9742	0.7784	0.7320	-0.4915	0.3271	0.0382
K_2	4.6894	1.6059	0.5410	0.9070	0.7515	0.4746	-0.7270	-0.9765	0.1567	0.3569
K_3	3.9835	1.8154	0.7204	1.2000	0.1868	0.7538	0.4693	0	0.2015	0.2501
K_4	4.1849	1.9992	0.7885	0.9353	0.3479	0.9989	0.9233	-0.8823	0.2015	0.2369
K_5	4.5736	1.9342	0.6787	0.9172	0.6589	0.9122	0.1911	-0.9425	0.1762	0.2702
K_6	3.2683	1.8901	0.7036	0.9446	-0.3854	0.8534	0.3574	-0.8514	0.2560	0.1508

Table 7: Objective functions and design variables of six representative designs from the Pareto optimal front.

Analysis of the Pareto optimal front

The Pareto optimal front contains large number of solutions and a classification is needed in order to study alternative designs. Here we have used hierarchical clustering algorithm (K-mean algorithm) in MATLAB to identify a representative set of six solutions. The objective functions and the design variables of these six designs are presented in Table 7. Besides, the objective functions of these designs are represented in the Pareto optimal front in Fig. 3.

The main conclusion that can be drown from the Table 7 is that the two objectives, the drag and the lift require different length of the front of the train L_1 in order to be low. For the minimal drag a long train is to prefer (see the cluster K_2) while the short train is advantageous for the minimal lift (see the cluster K_1). Another conclusion is that the optimal value of height c_2 seems to be fixed to values between approximately $0.9 - 1.0$. The only cluster having the c_2 value outside this range is cluster K_3. Thus fronts that are higher than $c_2 = 1.2$ are disadvantageous from the point of air resistance and stability (lift force). Comparing clusters K_2 and K_5 we see that the short length L_2 in combination with small ground clearance of the front of the train is particularly disadvantageous for the lift force.

Discussion and conclusions

The aim of this study was to investigate the use of surrogate shape optimization for vehicle aerodynamics. Although the technique was illustrated using simple two- dimensional vehicle it has been performed in such a way that can easily be applied for a general three-dimensional vehicles. It is obvious that the approach presented here is valuable and that if all the steps from geometric parameterization to validation of optimal design are carefully performed, its accuracy is high. Of course we have here only demonstrated that the optimal solution was found based on the CFD simulations performed with relatively inaccurate RANS turbulence model. This requires another test where the optimal design is simulated using an accurate time-dependent technique such as large eddy simulation (LES) or detached eddy simulation (DES). Such a test was not performed here mainly due to the character of the geometry, namely two-dimensional and the LES and DES can only be performed for three-dimensional computational domains.

There are still several issues that have to be addressed before this techniques can become an engineering tool. First unknown in this optimization work is of course the parameterization which should be done in (Computer Aided Design) CAD language using B-splines. However such a description of a three-dimensional geometry would result in a large number of design variables making the choice of important design variables even more difficult in order to decrease the number of expensive CFD calculations. From the point of aerodynamic engineer it is advantageous if the shape of the vehicle can be described in simple terms such as length, height or radius that later can be translated by the computer into a CAD model.

The choice of the DOE needs also to be investigated further. Although we have here used centered composite design (CCD) which was originally designed for physical experiments our numerical experiments are deterministic and there are number of designs that may be better suited for computer experiments. Examples of such designs are Latin hypercube sampling (LHS) and orthogonal arrays (OA) (see [9] for the review). There is a clear difference between the two design approaches (those for physical and computer experiments). As the DOE designed for physical experiments are taking into account the random variation in the sampled data, such a variation is irrelevant for the computer experiments as these are deterministic. This means for example that there is no need for duplicate designs in computer experiments.

Another issue that has to be addressed is the cost (in terms of men hours) of for the generation of the geometries and the computational grids for large number of designs. In the present work the author has use the ICEM-CFD package to generate all twenty five designs and the corresponding structured computational grids. Keeping in mind that generation of the computational grid around a realistic vehicle requires today several days (sometimes one to two weeks) this process has to be automated in order to make the optimization procedure feasible. There are already tools available for shape deformation of the computational grid which can help the tedious job of re-meshing the set of the designs.

The example demonstrated in the present work used a second order polynomial as a surrogate model. Although we have shown here that such a model is sufficient for the optimization of the two-dimensional geometry for drag and lift it is possible that higher order polynomial has to be used for three-dimensional geometries or other objective functions. Another types of surrogate models such as radial basis neural networks should be tested before an appropriate surrogate model is chosen for the general vehicle aerodynamics optimization.

Although there is a number of questions that have to be answered before the surrogate based optimization can become a general engineering tool for the aerodynamic optimization of vehicles, there is no doubt that it represents a valuable design strategy. With increase in computer power the steady CFD simulations will be replaced with more accurate unsteady simulations and thereby increase the accuracy of the response surface model substantially. Despite the promising computer development the use of the gradient-based search algorithms will be prohibited for many years to come (especially if time-dependent simulations are used). Using the surrogate based optimization together with time-dependent CFD simulations for the construction of the surrogate model will certainly become an optimization tool that is capable to compete with physical optimization in wind tunnels both in terms of cost and accuracy.

Acknowledgments

This work is financed by Banverket (Swedish National Rail Administration) under contract no.S05-3157/AL50 and it is a part of the project called Gröna Tåget. FLUENT Sweden and Bombardier Transportation are supporting the project.

References

1. N. V. Queipo, R. T. Haftka, W. Shyy, T. Goel, R. Vaidyanathan, and P. K. Tucker. Surrogate-based analysis and optimization. *Progress in Aerospace Sciences*, 41:1–28, 2005.
2. S. Krajnović and L. Davidson. Numerical Study of the Flow Around the Bus-Shaped Body. *ASME: Journal of Fluids Engineering*, 125:500–509, 2003.
3. S. Krajnović and L. Davidson. Flow Around a Simplified Car, Part 1: Large Eddy Simulation. *ASME: Journal of Fluids Engineering*, 127:907–918, 2005.
4. S. Krajnović and L. Davidson. Flow Around a Simplified Car, Part 2: Understanding the Flow. *ASME: Journal of Fluids Engineering*, 127:919–928, 2005.
5. S. Krajnović, H. Hemida, and B. Diedrichs. Time-dependent simulations for the directional stability of high speed trains under the influence of cross winds or cruising inside tunnels. In *FLUID DYNAMICS APPLICATIONS IN GROUND TRANSPORTATION:*.
6. S. Krajnović and L. Davidson. Influence of floor motions in wind tunnels on the aerodynamics of road vehicles, (in press). *Journal of Wind Engineering and Industrial Aerodynamics*, 2005.
7. H. Hemida, S. Krajnović, and L. Davidson. Large eddy simulations of the flow around a simplified high speed train under the influence of cross-wind. In *17th AIAA Computational Dynamics Conference*, Toronto, Ontario, Canada, 2005.
8. K. Deb, S. Agrawal, A. Pratap, and T. Mayarivan. A fast and elitist multiobjective genetic algorithm for multi-objective optimization: Nsga−ii. In *Parallel problem solving from nature VI conference, Paris, pp. 849-858*, 2000.
9. T. W. Simpson, J. D. Peplinski, P. N. Koch, and J. K. Allen. Metamodels for computer-based engineering design: Survey and recommendations. *Engineering with Computers*, 17:129–150, 2001.